

A. I. Levon<sup>1</sup>, P. Alexa<sup>2</sup>, S. Pascu<sup>3</sup>, P. G. Thirolf<sup>4</sup>

<sup>1</sup> Institute for Nuclear Research, National Academy of Sciences of Ukraine, Kyiv, Ukraine

<sup>2</sup> Institute of Physics and Institute of Clean Technologies, Technical University of Ostrava, Czech Republic

<sup>3</sup> H. Hulubei National Institute of Physics and Nuclear Engineering, Bucharest, Romania

<sup>4</sup> Fakultät für Physik, Ludwig-Maximilians-Universität München, Garching, Germany

## TO THE NATURE OF 0<sup>+</sup> EXCITATIONS IN DEFORMED NUCLEI OF ACTINIDES

The excitation spectra in the deformed nucleus <sup>232</sup>U have been studied by means of the (p, t) reaction. 0<sup>+</sup> assignments for 13 excited states and up to spin 6<sup>+</sup> for other states are made from the angular distributions of tritons and the coupled-channel approximation analysis. Sequences of states are selected which can be treated as rotational bands. Moments of inertia have been derived from these sequences, whose values may be considered as evidence of the two- or one-phonon nature of these 0<sup>+</sup> excitations. Experimental data are compared with interacting boson model (IBM) and quasiparticle-phonon model (QPM) calculations.

*Keywords:* 0<sup>+</sup> states, collective bands, moments of inertia, nuclear models.

### Introduction

Most of the experimental studies [1 - 6] using the two neutrons transfer reaction were limited to measuring the energies and excitation cross sections of 0<sup>+</sup> states. Therefore, they provided only the trend of changes in the nuclei contributing to such excitations in a wide range of deformations. More information from the (p, t) experiments was given in [7, 8]. They report data on spins and cross sections for all states observed in the (p, t) reaction. This allowed to extract information about the moments of inertia for the bands built on the 0<sup>+</sup> states. All these experimental studies contributed to the development of theoretical calculations, which explain some of the features of the 0<sup>+</sup> excitation spectra. Some publications have dealt with the microscopic approach, such as quasiparticle-phonon model (QPM) [9, 10], but the majority of studies used the phenomenological model of interacting bosons (IBM) [11, 12]. These approaches have been used also in [6 - 8]. Nevertheless, the nature of multiple 0<sup>+</sup> excitations in even nuclei is still far from being understood.

In this paper we analyze the experimental data from the <sup>234</sup>U(p, t)<sup>232</sup>U reaction described in the article [13]. Conclusion on the moments of inertia is made from the collective bands built on the base of the DWBA analysis of the experimental data. Different microscopic approaches are used to obtain a detailed information on the properties of 0<sup>+</sup> states excited in the (p, t) reaction. The IBM-*spdf* calculations have been applied to explain the experimental data too.

### Collective bands and moments of inertia in <sup>232</sup>U

Aiming to get more information on the excited states in <sup>232</sup>U, especially on the moments of inertia for

the 0<sup>+</sup> states, we have attempted to identify those sequences of states, which show the characteristics of a rotational band structure. An identification of the states attributed to rotational bands can be made on the basis of the following conditions: a) the angular distribution for a band member candidate is fitted by DWBA calculations for its expected spin; b) the transfer cross section in the (p, t) reaction to states in the potential band has to decrease with increasing spin; c) the energies of the states in the band can be fitted approximately by the expression for a rotational band  $E = E_0 + AI(I + 1)$  with a small and smooth variation of the inertial parameter  $A$ . Collective bands identified in such a way are listed in Table 1. The procedure can be justified, since some sequences meeting the above criteria are already known to be rotational bands from gamma-ray spectroscopy [14]. In Fig. 1 we present moments of inertia (MI) obtained by fitting the level energies of the bands displayed in Table 1 by the expression for energies of the close-lying levels, i.e., they were determined for the band members using the ratio of  $\Delta E$  and  $\Delta[I(I + 1)]$ , thus saving the spin dependence of the MI.

*Negative parity states.* Unlike the thorium isotopes [7, 8], some uncertainties in formation of the bands are met for <sup>232</sup>U. At the beginning, a few comments follow about the lowest negative-parity states, usually interpreted as having an octupole vibrational character. They are one-phonon octupole excitations, forming a quadruplet of states with  $K^\pi = 0^-, 1^-, 2^-, 3^-$  and are the bandheads for the rotational bands. The  $K^\pi = 0^-$  band is reliably established [14] and confirmed by the present study. There are two states with  $J^\pi = 2^-$  at 1016.8 and 1173.1 keV, which may be members of bands with  $K^\pi = 1^-$  and  $K^\pi = 2^-$ . The level at 1146.3 keV has

© A. I. Levon, P. Alexa, S. Pascu, P. G. Thirolf, 2016

**Table 1. The sequences of states (in units of keV) which can belong to rotational bands (from the CHUCK fit, the (p, t) cross sections and the inertial parameters). More accurate values of energies are taken from the first two columns of Table 1 in [13]**

| 0 <sup>+</sup> | 1 <sup>+</sup> | 2 <sup>+</sup> | 3 <sup>+</sup> | 4 <sup>+</sup> | 5 <sup>+</sup> | 6 <sup>+</sup> | 7 <sup>+</sup> | 8 <sup>+</sup> |
|----------------|----------------|----------------|----------------|----------------|----------------|----------------|----------------|----------------|
| 0.0            |                | 47.6           |                | 156.6          |                | 322.7          |                | 541.1          |
| 691.4          |                | 734.6          |                | 833.1          |                | 984.9          |                | 1186.6         |
|                |                | 866.8          | 911.5          | 970.7          |                | (1132.7)       |                |                |
|                |                | 1132.7         |                | 1226.8         |                | 1372.0         |                |                |
| or             |                |                |                | 1226.8         |                | 1372.0         |                |                |
|                |                |                |                | 1194.0         |                | 1314.8         |                |                |
| 927.3          |                | 967.6          |                |                |                |                |                |                |
| 1277.2         |                | 1301.4         |                | 1361.5         |                | 1460.4         |                |                |
|                |                | 1489.2         |                | 1572.9         |                | 1700.5         |                |                |
| 1482.2         |                | 1520.4         |                | 1605.4         |                | 1737.4         |                |                |
| 1569.0         |                | 1600.2         |                | 1673.2         |                | 1790.8         |                |                |
|                |                | 1647.7         |                | 1744.4         |                | 1880.8         |                |                |
| 1797.0         |                | 1838.6         |                |                |                |                |                |                |
| 1821.8         |                | 1870.9         |                |                |                |                |                |                |
| 1861.0         |                | (1915.2)       |                |                |                |                |                |                |
| 1931.0         |                | 1970.7         |                | 2068.6         |                |                |                |                |
| or             |                |                |                |                |                |                |                |                |
| 1931.0         |                | 1977.8         |                |                |                |                |                |                |
|                |                | 2059.8         |                | 2135.9         |                | 2254.4         |                |                |
|                |                | 2146.5         |                | 2231.3         |                |                |                |                |
|                |                | 2203.8         |                | 2312.2         |                |                |                |                |
|                |                | 2418.8         |                | 2527.2         |                |                |                |                |
|                |                | 2673.5         |                | 2754.3         |                | 2878.3         |                |                |
|                |                | 2779.1         |                | 2889.8         |                | 3058.3         |                |                |
|                |                | 2791.0         |                | 2899.2         |                |                |                |                |
| 2917.4         |                | 2959.7         |                |                |                |                |                |                |
|                |                |                |                |                |                |                |                |                |
| 0 <sup>-</sup> | 1 <sup>-</sup> | 2 <sup>-</sup> | 3 <sup>-</sup> | 4 <sup>-</sup> | 5 <sup>-</sup> | 6 <sup>-</sup> | 7 <sup>-</sup> | 8 <sup>-</sup> |
|                |                |                |                |                |                |                |                |                |
|                | 563.2          |                | 629            |                | 746.8          |                | 915.2          |                |
|                |                | 1016.8         | 1050.9         | 1098.2         | 1155.4         |                |                |                |
|                | (1141.5)       | 1173.1         | 1211.3         |                | (1321.8)       |                |                |                |
|                |                |                | 1264.8         |                | 1391.7         |                |                |                |
|                |                |                | 1679.8         |                | 1758.9         |                |                |                |

been proposed as a band head of the  $K^\pi = 1^-$  band from the observation of  $\gamma$  ray with this energy [14]. The corresponding line in the triton spectra is absent. After our firm assignment of spin  $4^+$  to the state at 1194.1 keV, this proposal has to be rejected since the 1146.3 keV transition should be referred to the decay of this level to the  $2^+$  level at 47.6 keV. At the same time, a line in the triton spectra is observed at 1141.5 keV, and the spin of the corresponding state is assigned tentatively as  $1^-$ . Considering this level as the bandhead for the  $1^-$  band with two levels known from previous studies [14], the moments of inertia can be calculated. The procedure described above can not be applied in this case because of the mixing by the Coriolis interaction. A simplified expression for the band energies can be used in the analysis (for details see [8])

$$E(I, K^\pi = 1^-) \sim E_1 + (A_1 + B)I(I+1) \quad \text{for } I \text{ odd}$$

$$E(I, K^\pi = 1^-) \sim E_1 + A_1 I(I+1) \quad \text{for } I \text{ even} \quad (1)$$

Considering  $E_1$ ,  $A_1$  and  $B$  as parameters, we obtained from the energies of three levels  $E_1 = 1127.3$  keV,  $A_1 = 7.63$  keV and  $B = -0.47$  keV. This corresponds to a moment of inertia of  $65.5$  MeV<sup>-1</sup> (see Fig. 1). The difference relative to the moment of inertia of the  $0^+$  band is quite large, and the energy of 1173.1 keV of the  $2^-$  level of thus assumed  $1^-$  band is much higher than the energy of 1016.8 keV of the  $2^-$  level of the assumed the  $2^-$  band (should be the opposite). If, however, we consider the 1173.1 keV state as the bandhead of the  $K^\pi = 2^-$  band, then the moment of inertia is determined as  $78.5$  MeV<sup>-1</sup> close

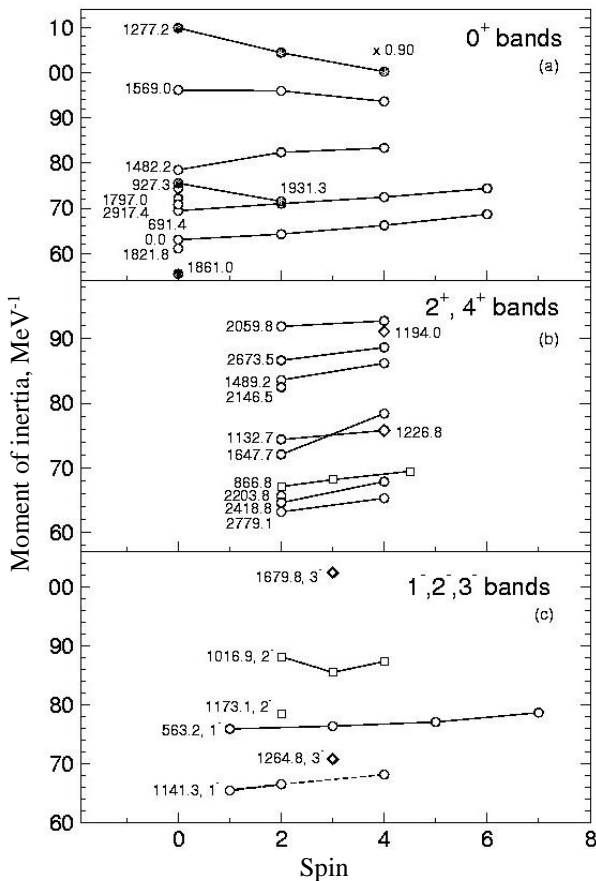


Fig. 1. Moments of inertia for the bands in  $^{232}\text{U}$ , as assigned from the angular distributions from the  $^{234}\text{U}(p, t)^{232}\text{U}$  reaction. Values of  $J/h^2$  are given. In the graph, they are placed at spins of the first state from the two states used in the calculations of every value. Numbers are given for the energy levels in keV.

to the moment of inertia of the  $K^\pi = 0^-$  band. Although some ambiguity remains, the level  $3^-$  at 1264.8 keV can be proposed as the bandhead of the  $K^\pi = 3^-$  band.

In a more accurate model [31], that takes into account the Coriolis interaction between all octupole bands, one can fit 11 parameters (bandhead energies, rotation parameters and Coriolis intrinsic matrix elements between bandheads) to the experimental energies. The former level assignment gives  $E_0 = 551.0$  keV,  $E_1 = 1136$  keV,  $E_2 = 1006$  keV,  $E_3 = 1241$  keV with  $\chi^2 = 0.97$ , while the latter gives a slightly better value of  $\chi^2 = 0.63$  and reasonable values of the fitted energies  $E_0 = 551.6$  keV,  $E_1 = 987.4$  keV,  $E_2 = 1158$  keV,  $E_3 = 1240$  keV. However, the predicted  $1^-$  bandhead at 994 keV is not observed experimentally.

*The  $2^+$ ,  $4^+$  and  $6^+$  states.* States with spins and parities firmly assigned as  $2^+$  excitations dominate in the triton spectra. Some of them are assigned as members of  $K^\pi = 0^+$  bands and others probably are

band heads and the levels with spins  $4^+$  and even  $6^+$  are identified as possible members of these bands. Using the analysis of the  $\gamma$ -spectra [14] one can identify the 866.8 keV state as the bandhead of the  $\gamma$ -vibrational band with members 911.5 and 970.7 keV. A possible continuation of this band can be the 1132.7 keV state, since for this state the typical  $2^+$  angular distribution is distorted by a possible admixture of a  $6^+$  state (it might be a doublet of  $2^+$  and  $6^+$  states). The 1132.7 keV state was tentatively identified as the band head of the  $K^\pi = 2^+$  in [15] through the analysis of the  $\gamma$  spectra. The  $4^+$  states at 1226.8 keV and the  $6^+$  state at 1372.0 keV could be proposed to be members of this band. However, the cross section for the  $4^+$  state exceeds the one for the  $2^+$  state, in contrast to the above conditions. Therefore, the  $K^\pi = 4^+$  band is offered as an option.

*The  $0^+$  states.* For the state at the energy of 927.3 keV assigned in [16] (in this study as a  $0^+$  state) no members of the band were observed in the  $(p, t)$  reaction. The energy 967.6 keV was accepted for the  $2^+$  band component as suggested in [16]. The  $0^+$  state at 1277.2 keV is strongly excited and the members of the assumed band have to be excited too. A clear sequence of states is observed with a spin assignment of  $2^+$ ,  $4^+$  and  $6^+$ , as seen in Table 1, but moments of inertia determined from this sequence are very high (124  $\text{MeV}^{-1}$  from the  $2^+$  and  $0^+$  state energy difference) and are decreasing as a function of spin. Other possible sequences do not satisfy the conditions set forth above. A possible explanation for such a behavior was suggested in [8] but it is hardly applicable in this case.

The structure of this state is assumed to be different from other collective states. To some extent the same remark can be attributed to the band probably built on the  $0^+$  state at 1569.0 keV, whose moment of inertia decreases as a function of spin, though weakly. The  $0^+$  states at 1797.0, 1821.8 and 1861.0 keV are also strongly excited and the excitation of other members of the assumed bands have to be seen in the  $(p, t)$  reaction. At least the  $2^+$  states can be attributed to such bands built on the  $0^+$  states at 1797.0 and 1821.8 keV. For the  $0^+$  state at 1861.0 keV, no prolongation of the band is clearly visible in the triton spectra. Only the unlikely assumption can be made that the corresponding line is hidden under the 1915.2 keV line, but the moment of inertia of 55.4  $\text{MeV}^{-1}$  by this assumption is much less than the one for the ground state. An ambiguous situation is met also for the  $0^+$  state at 1931.0 keV, whose excitation is only slightly weaker than the first excited state at 691.4 keV. Two different sequences can be assumed for the band built on this state, but for both the moment of inertia is decreasing with spin. As it was noted already, the angular distribution for the

state at 2917.4 keV differs considerably from all others and can be fitted only by the calculation for transfer of the  $(1j_{15/2})^2$  neutron configuration.

**Moments of inertia (MI).** The moment of inertia of the g.s. of  $^{232}\text{U}$  as  $63 \text{ MeV}^{-1}$  is much higher than in  $^{228}\text{Th}$  and  $^{230}\text{Th}$ . The  $K^\pi = 0^-$  band with the bandhead  $1^-$  at 563.2 keV is well defined, it exhibits an MI increase of about 20 % and can serve as orientation for such excitations. The assumption that the  $2^-$  level at 1173.1 keV belongs to the  $K^\pi = 1^-$  band is not confirmed by the present analysis (see above). If, however, we assume that the state at 1173.1 keV is the bandhead of the  $K^\pi = 2^-$  band, then the MI determined from the  $3^-$  and  $2^-$  energy difference is  $78.5 \text{ MeV}^{-1}$ , slightly higher than the MI of the  $K^\pi = 0^-$  band. Although the ambiguity remains, the level  $2^-$  at 1016.9 keV is the member of the  $K^\pi = 1^-$  band (with the non-observed  $1^-$  level) and the  $3^-$  at the level 1264.8 keV can be proposed as the bandhead of the  $K^\pi = 3^-$  band.

Unlike in  $^{228}\text{Th}$  and  $^{230}\text{Th}$ , the MI of the bands built on the excited  $0^+$  states in  $^{232}\text{U}$  are not much higher than those for the g.s. band. Only two bands, starting at 1227.2 and 1569.0 keV, have a significant excess of the MI. The principal difference is that the first excited  $0^+$  state in  $^{232}\text{U}$  seems to be a  $\beta$ -vibrational state. The results of the analysis of  $\gamma$ -spectra and the MI value close to the one of the g.s. give evidence for such a conclusion. In addition, the first excited  $0^+$  state in  $^{228}\text{Th}$  [8] as well as in  $^{240}\text{Pu}$  [17] have perhaps an octupole two-phonon nature. The first excited (possible  $\beta$ -vibrational) state in  $^{232}\text{U}$  is most strongly excited, just the same as the the first excited (octupole two-phonon) states in  $^{228}\text{Th}$  and  $^{240}\text{Pu}$ , and the first excited state with a more complicated phonon structure in  $^{230}\text{Th}$  [7]. In  $^{232}\text{U}$ , the state at 927.3 keV was suggested [16] to be an octupole two-phonon excitation. It is confirmed by large values of the  $B(E1)/B(E2)$  ratio calculated using the data of the  $\gamma$ -intensities for transitions from  $0^+$  and  $2^+$  levels of this band to the levels of the  $0^-$  and g.s. bands [16] (see discussion below and Tables 2 and 4).

The MI of the 927.3 keV band confirms this assignment, though it is only 16 % larger than that of the g.s., compared to a larger excess of 36 and 23 % for  $^{228}\text{Th}$  and  $^{230}\text{Th}$  respectively. All these facts indicate that the strong population of the first excited  $0^+$  states does not allow to identify their phonon structure.

The value of the MI for the band built on the  $2^+$  state at 866.8 keV is close to the one for a possible  $\beta$ -vibration band (they are only 6 and 8 % larger than those of the g.s. band), thus confirming its interpretation as the  $\gamma$ -vibrational band. As for the experi-

mental evidence of the nature of other  $0^+$  states, we derived only values of the MI from the sequences of states treated as rotational bands and hence rather tentative conclusions can be drawn about their structure. In contrast to  $^{230}\text{Th}$  [7], for which they are distributed almost uniformly over the range until 1.80 of the g.s. value (equal to  $56 \text{ MeV}^{-1}$ ) and to  $^{228}\text{Th}$ , for which most of values are in the range of  $1.35 \div 1.85$  of the g.s. value (equal to  $52 \text{ MeV}^{-1}$ ), most of the MI values of the  $0^+$  states in  $^{232}\text{U}$  do not exceed the value of 1.27 of the g.s. value (equal to  $63 \text{ MeV}^{-1}$ ). This fact shows that the corresponding states are having perhaps the quadrupole one-phonon or two-phonon nature.

### IBM calculations

The Interacting Boson Model describes the low-lying positive and negative parity states by treating the valence nucleons in pairs as bosons. The positive parity states are described by introducing  $s$  and  $d$  bosons, which carry angular momentum of  $L^\pi = 0^+$  and  $L^\pi = 2^+$  respectively, while the negative parity states can be calculated by additionally including  $p$  and  $f$  bosons having  $L^\pi = 1^-$  and  $L^\pi = 3^-$  respectively. In the present paper the IBM-1 version of the model is used, which means that no distinction is made between protons and neutrons [18]. Full IBM-*spdf* calculations have been previously done with success in [19 - 21].

The octupole degree of freedom is well known for playing a major role in the actinide region [22, 23]. In fact, octupole correlations have been predicted to be found in the  $Z \sim 88$  and  $N \sim 134$  region [24]. They have attracted a lot of experimental investigations centered on energy spectra and transition probabilities [25]. The low-lying properties of these nuclei have been interpreted using a series of theoretical models, including the IBM [20, 21], which mainly concentrated on the study of electromagnetic decay properties. In the last years, several nuclei in this region were investigated using the (p, t) reaction and the transfer intensities became available too [7, 8, 17]. Therefore, several models tried to describe the complete experimental situation [8, 10, 17].

As presented also in this paper, an increased number of  $0^+$  excitations have been populated in the previous two-neutron transfer experiments with a rather high intensity [7, 8, 17]. Since some of these states strongly decay to the negative parity states, it is believed that the quadrupole and octupole degrees of freedom are closely connected to these excitations. In the IBM, such  $0^+$  states have been interpreted as having a double octupole character [8, 17]. Although this simple picture can be criticized, the IBM has been proved to reasonably describe simultaneously

the electromagnetic and transfer properties. In order to reproduce the experimental features, one has to abandon the description of the nuclei using a simplified Hamiltonian, which is suited to describe mainly electromagnetic data. However, such calculations were found to be completely failed to reproduce the  $(p, t)$  spectroscopic factors by predicting a transfer strength of 1 % of that of the ground state, while experimentally the summed transfer intensity amounts to about 80 % in this region. The solution seems to be the introduction of the second-order  $O(5)$  Casimir operator in the Hamiltonian, which allows for a far better description of the complete experimental data.

$$\begin{aligned} \hat{Q}_{spdf} = \hat{Q}_{sd} + \hat{Q}_{pf} = & (\hat{s}^\dagger \tilde{d} + \hat{d}^\dagger \hat{s})^{(2)} + \chi_{sd}^{(2)} (\hat{d}^\dagger \tilde{d})^{(2)} + \frac{3\sqrt{7}}{5} [(p^\dagger \tilde{f} + f^\dagger \tilde{p})]^{(2)} + \\ & + \chi_{pf}^{(2)} \left\{ \frac{9\sqrt{3}}{10} (p^\dagger \tilde{p})^{(2)} + \frac{3\sqrt{42}}{10} (f^\dagger \tilde{f})^{(2)} \right\}. \end{aligned} \quad (3)$$

The quadrupole electromagnetic transition operator takes the form

$$\hat{T}(E2) = e_2 \hat{Q}_{spdf}, \quad (4)$$

where  $e_2$  represents the boson effective charge.

The  $E1$  transitions are described in the IBM by a linear combination of the three allowed one-body interactions

$$\begin{aligned} \hat{T}(E1) = e_1 [\chi_{sp}^{(1)} (s^\dagger \tilde{p} + p^\dagger \tilde{s})^{(1)} + (p^\dagger \tilde{d} + d^\dagger \tilde{p})^{(1)} + \\ + \chi_{df}^{(1)} (d^\dagger \tilde{f} + f^\dagger \tilde{d})^{(1)}], \end{aligned} \quad (5)$$

where  $e_1$  is the effective charge for the  $E1$  transitions, and  $\chi_{sp}^{(1)}$  and  $\chi_{df}^{(1)}$  are model parameters.

At this point, one has to introduce an additional term in order to describe the connection between states with no  $(pf)$  content with those having  $(pf)^2$  components. This term is very useful to describe both the  $E2$  transitions, and in addition, the transfer strength between such states. Therefore, the same dipole-dipole interaction term is introduced in the present calculations as previously used in. [8, 19, 21]:

$$\hat{H}_{int} = \alpha \hat{D}_{spdf}^\dagger \cdot \hat{D}_{spdf} + H.c., \quad (6)$$

where

$$\begin{aligned} \hat{D}_{spdf} = -2\sqrt{2} [p^\dagger \tilde{d} + d^\dagger \tilde{p}]^{(1)} + \sqrt{5} [s^\dagger \tilde{p} + p^\dagger \tilde{s}]^{(1)} + \\ + \sqrt{7} [d^\dagger \tilde{f} + f^\dagger \tilde{d}]^{(1)} \end{aligned} \quad (7)$$

is the dipole operator arising from the  $0(4)$  dynamical symmetry limit, which does not conserve separately the number of positive and negative parity bosons [28, 29].

These calculations were performed in the *spdf* IBM-1 framework using the Extended Consistent Q-formalism (ECQF) [26]. The IBM Hamiltonian employed in the present paper is given by

$$\begin{aligned} \hat{H}_{spdf} = \epsilon_d \hat{n}_d + \epsilon_p \hat{n}_p + \epsilon_f \hat{n}_f + \kappa (\hat{Q}_{spdf} \cdot \hat{Q}_{spdf})^{(0)} + \\ + a_3 [(\hat{d}^\dagger \tilde{d})^{(3)} \cdot (\hat{d}^\dagger \tilde{d})^{(3)}]^{(0)}, \end{aligned} \quad (2)$$

where  $\epsilon_d$ ,  $\epsilon_p$ , and  $\epsilon_f$  are the boson energies and  $\hat{n}_p$ ,  $\hat{n}_d$ , and  $\hat{n}_f$  are the boson number operators. In the *spds* model, the quadrupole operator is considered in [27]:

The goal of the present paper is to describe simultaneously both the existing electromagnetic and the transfer strength data. To achieve the goal, two-neutron transfer intensities between the ground state of the target nucleus and the excited states of the residual nucleus were also calculated. The  $L = 0$  transfer operator has the following form in the IBM:

$$\begin{aligned} \hat{P}_v^{(0)} = (\alpha_p \hat{n}_p + \alpha_f \hat{n}_f) \hat{s} + \\ + \alpha_v \left( \Omega_v - N_v - \frac{N_v}{N} \hat{n}_d \right)^{\frac{1}{2}} \left( \frac{N_v + 1}{N + 1} \right)^{\frac{1}{2}} \hat{s}, \end{aligned} \quad (8)$$

where  $\Omega_v$  is the pair degeneracy of the neutron shell,  $N_v$  is the number of neutron pairs,  $N$  is the total number of bosons; and  $\alpha_p$ ,  $\alpha_f$ , and  $\alpha_v$  are constant parameters. In this configuration, the  $L = 0$  transfer operator contains additional terms besides the leading order term (third term) [18], which ensures a non-vanishing transfer intensity to the states with the  $(pf)^2$  configuration.

The calculations were performed by using the computer code OCTUPOLE [29] which allows up to three negative parity bosons. The following parameters in the IBM Hamiltonian have been used:  $\epsilon_d = 0.27$  MeV,  $\epsilon_p = 1.14$  MeV,  $\epsilon_f = 0.95$  MeV,  $\kappa = -13$  keV, and  $a_3 = 0.026$  MeV, which ensures a good reproduction of the low-energy states. The interaction strength is given by the  $\alpha$  parameter and is chosen to have a very small value,  $\alpha = 0.0005$  MeV, similar to that obtained in [20, 21]. Therefore, the last has a very small influence on the level energies.

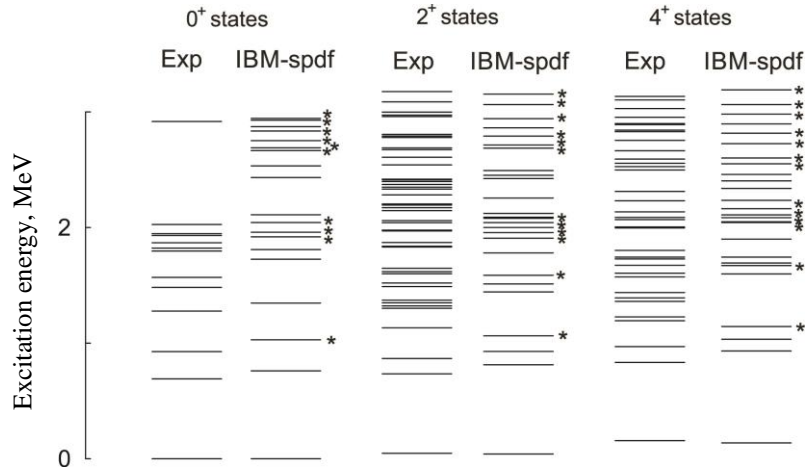


Fig. 2. Energies of all excited  $0^+$ ,  $2^+$ , and  $4^+$  states experimentally assigned in  $^{232}\text{U}$  in comparison with IBM-*spdf* calculations. The states containing 2 *pf* bosons in their structure and assumed to have a double dipole/octupole character are marked with an asterisk.

The most important result of these (p, t) transfer experiments is the fact that they reveal a large number of  $0^+$  states, the presence of such states at higher excitation energies being the subject of intensive theoretical investigations. Therefore, we present in Fig. 2 the full spectrum of experimental excited  $0^+$  states in comparison with the corresponding calculated values. As the result, the IBM calculations show the existence of 19 states of the type  $0^+$  up to an excitation energy of 3 MeV in comparison with 13 states excited in the experiment about in the same energy range. The calculated distribution of  $0^+$  states is very similar to the experimental one up to around 2 MeV. The situation is completely different between 2 and 3 MeV, where a large gap is seen in the experiment up to 2.9 MeV, while the IBM yields an increased number of states with increasing excitation energy. In the experiment, we can speculate that in this region the  $0^+$  states carry very small transfer strengths. Therefore, the sensitivity of our experiment was not sufficient to discriminate individual states. Most of the calculated excitations in this energy range are having two *pf* bosons in their structure (states marked with asterisk), and hence manifested a double dipole/octupole structure [20]. Although it is very interesting that IBM describes simultaneously both the electromagnetic and transfer, this is most likely not the only mechanism providing an increased number of  $0^+$  states, and therefore, we cannot make a definite conclusion on the nature of these excitations based only on these limited experimental data. To support such a claim, more experimental information is needed, and in particular, the *E1* and *E3* transition probabilities to the negative parity states. In Fig. 2, the  $2^+$  and  $4^+$  levels revealed in the present experiment are also compared with the results of the IBM calculations. The experiment revealed 40 firmly assigned excited  $2^+$  states and 26 solid assigned

excited  $4^+$  states up to 3.2 MeV. In the same energy range, the calculations produced 26 excited  $2^+$  and 26  $4^+$  states.

Since the octupole degree of freedom plays an important role in this mass region, it is crucial for a model to describe simultaneously at least the *B(E1)* and the *B(E1)/B(E2)* ratios, if the reduced transition probabilities have not been measured. In the IBM, the *E1* and *E2* transitions are calculated by Eqs. (5) and (4) respectively. We have used  $\chi_{sd}^{(2)} = -1.32$ ,  $\chi_{pf}^{(2)} = -1$  as the quadrupole operator parameters and  $\chi_{sp} = \chi_{df} = -0.77$  for the parameters in Eq. (5). The remaining parameters are the effective charges and are used to set the scale of the corresponding transitions:  $e_1 = 0.0065$  efm and  $e_2 = 0.184$  eb.

Table 2. Experimental and calculated *B(E1)/B(E1)* (from the  $0_1^-$  state) and *B(E1)/B(E2)* (from the  $0_3^+$  state) transitions ratios in  $^{232}\text{U}$ . The parameters of the *E1* operator are fitted to the experimental data available. The *B(E1)/B(E2)* ratios are given in units of  $10^{-4} \cdot \text{b}^{-1}$

| $K^\pi$            | $E_i$ , keV | $J_i$ | $J_{f1}$ | $J_{f2}$ | Exp.               | IBM  |
|--------------------|-------------|-------|----------|----------|--------------------|------|
|                    |             |       |          |          | <i>B(E1)/B(E1)</i> |      |
| $0_1^-$            | 563         | $1^-$ | $2_1^+$  | $0_1^+$  | 1.89(8)            | 1.89 |
|                    | 629         | $3^-$ | $4_1^+$  | $2_1^+$  | 1.19(5)            | 1.17 |
|                    | 747         | $5^-$ | $6_1^+$  | $4_1^+$  | 0.94(8)            | 0.97 |
| <i>B(E1)/B(E2)</i> |             |       |          |          |                    |      |
| $0_3^+$            | 927         | $0^+$ | $1_1^-$  | $2_1^+$  | 44(7)              | 58   |
|                    | 968         | $2^+$ | $1_1^-$  | $0_1^+$  | 150(30)            | 122  |
|                    |             | $2^+$ | $1_1^-$  | $2_1^+$  | 45(1)              | 85   |
|                    |             | $2^+$ | $1_1^-$  | $4_1^+$  | 24(1)              | 47   |
|                    |             | $2^+$ | $3_1^-$  | $0_1^+$  | 337(68)            | 167  |
|                    |             | $2^+$ | $3_1^-$  | $2_1^+$  | 101(3)             | 117  |
|                    |             | $2^+$ | $3_1^-$  | $4_1^+$  | 54(1)              | 65   |

The  $B(E1)/B(E2)$  ratios discussed in Table 2 belong to the  $K^\pi = 0_3^+$  band (the believed double octupole phonon band). All the states belonging to this band are having  $(pf)^2$  bosons in their structure in the IBM calculations. They are supposed to have a double octupole phonon character. The agreement in Table 2 between experiment and calculations is remarkably good, that gives even more confidence in the structure proposed by the IBM. If other excited  $0^+$  levels decay to the negative parity states, one would need the crucial information about the decay pattern of these levels. This can be achieved by future  $(p, \gamma)$  and  $(n, n'\gamma)$  experiments and we stress here the necessity of performing such delicate investigations.

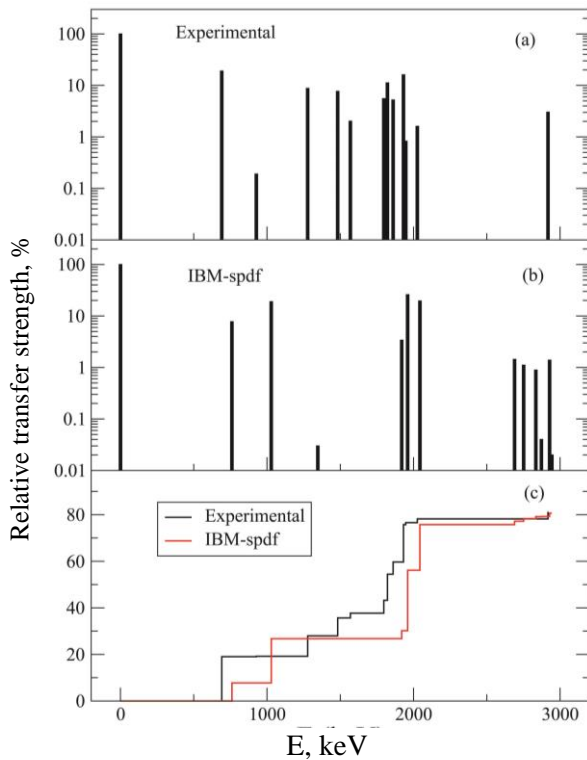


Fig. 3. Comparison between the experimental (both firm and tentatively assigned states are included in the figure) two-neutron transfer intensities (a) for the  $0^+$  states and the IBM results (b). The experimental versus computed running sum of the  $(p, t)$  strengths (c).

The experimental integrated two-neutron transfer intensities are displayed in Fig. 3, a. In contrast to  $^{228,230}\text{Th}$  where the spectrum is dominated by a single state with high cross section of about 15 - 20 % of that of the ground state, the transfer intensity in  $^{232}\text{U}$  goes not only to the first excited  $0^+$  state, but also to a group of states around 2 MeV, which carries more than 30 %. In the IBM (see Fig. 3, b), the transfer intensity is also split between the first two excited  $0^+$  states and a group of  $0^+$  excitations around 2 MeV. For easy comparison with the experimental data, one has to look also at the summed transfer intensity; which is presented in

Fig. 3, c for both the experimental and the calculated values. The main characteristics of the experimental transfer distribution are reproduced, namely the increased population of two groups of  $0^+$  excitations around 1 and 2 MeV, but the IBM fails to give a detailed explanation of the individual states. To perform the IBM calculations, the parameters from Eq. (8) were estimated from the fit of the known two-neutron transfer intensities (integrated cross sections) in Table 1 in [13]. The values employed in the present calculations are  $\alpha_p = 0.51$  mb/sr,  $\alpha_f = -0.45$  mb/sr, and  $\alpha_1 = 0.013$  mb/sr.

### QPM calculations

To obtain a detailed information on the properties of the states excited in the  $(p, t)$  reaction, a microscopic approach is necessary. The first transparent step in this respect is the well-known Quasiparticle-phonon model (QPM) [30]. The ability of the QPM to describe multiple  $0^+$  states (energies,  $E2$  and  $E0$  strengths, two-nucleon spectroscopic factors) was demonstrated for  $^{158}\text{Gd}$  [9]. In a subsequent paper the QPM was applied to the microscopic structure of  $0^+$  states in  $^{168}\text{Er}$  and three actinide nuclei ( $^{228}\text{Th}$ ,  $^{230}\text{Th}$  and  $^{232}\text{U}$ ) [10]. Single particle basis states up to 5 MeV were generated by a deformed axially-symmetric Woods-Saxon potential. Two-body potentials were represented by a monopole plus multipole pairing interaction and isoscalar and isovector multipole-multipole interactions. Two-phonon states were calculated for multipolarities  $\lambda = 2 - 5$ . These calculations are also used to compare to the present detailed analysis of the experimental data for  $^{232}\text{U}$ . As for the theoretical basis of the calculations, we refer to the publications [10, 30].

The  $(p, t)$  normalized relative transfer spectroscopic strengths in the QPM are expressed as ratios

$$S_n(p, t) = \left[ \frac{\Gamma_n(p, t)}{\Gamma_0(p, t)} \right]^2, \quad (9)$$

where the amplitude  $\Gamma_n(p, t)$  includes the transitions between the  $^{234}\text{U}$  ground state and one-quadrupole  $K = 0$  phonon components of the  $^{232}\text{U}$  wave function. The amplitude  $\Gamma_0(p, t)$  refers to the transition between the  $^{234}\text{U}$  and  $^{232}\text{U}$  ground states. The selected normalization assures that  $S_0(p, t) = 100$  for the ground state transition.

To see the role of the two-phonon and pairing-vibrational excitations in the QPM calculations, we performed simple QPM (SQPM) calculation using the Nilsson potential plus monopole pairing interaction (Nilsson parameters  $\kappa$  and  $\mu$  are taken from [31], deformation parameters  $\epsilon_2 = 0.192$ ,

$\epsilon_4 = -0.008$  and pairing gaps  $\Delta_p = 0.706$  MeV,  $\Delta_n = 0.602$  MeV for  $^{232}\text{U}$  and  $\epsilon_2 = 0.200$ ,  $\epsilon_4 = -0.073$  and pairing gaps  $\Delta_p = 0.738$  MeV,  $\Delta_n = 0.582$  MeV for  $^{234}\text{U}$  from [32, 33]) plus isoscalar and isovector quadrupole-quadrupole and octupole-octupole interactions. In these calculations only one-phonon RPA states were taken into account. Energies of two-quasiparticle  $0^+$  states were estimated from the BCS theory. The model predicts 15 neutron two-quasiparticle states of the structure  $\alpha_q^\dagger \alpha_q^\dagger$  below 4 MeV that correspond to broken neutron pairs sensitive to two-neutron transfer. The energies and normalized relative transfer strengths are shown in Fig. 4, *a* for  $S_n(p, t) \geq 0.01$ . They are compared to the experimental energies and relative transfer strengths. It is evident that the two-quasiparticle  $0^+$  states represent only a small contribution to the total relative transfer strength (see Fig. 4, *c*).

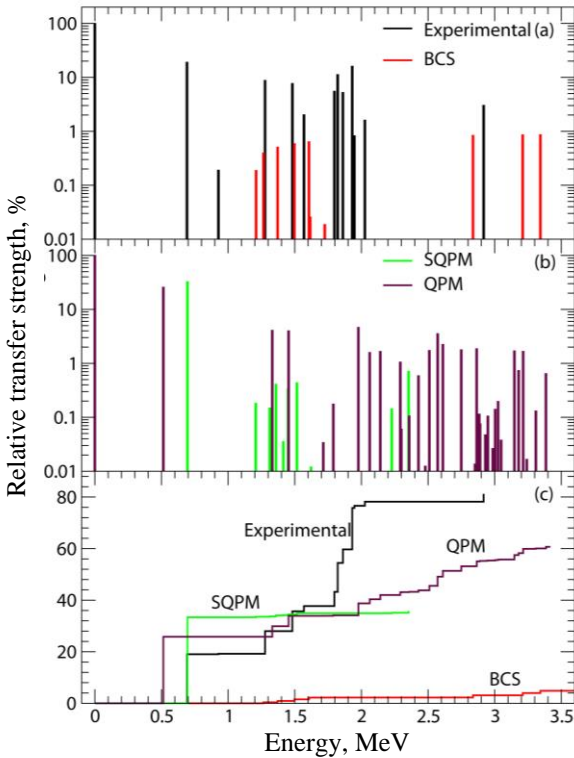


Fig. 4. Comparison of experimental and BCS (*a*), SQPM and QPM (*b*)  $0^+$  ( $p, t$ ) normalized relative strengths. The value for the  $0^+_{g.s.}$  is normalized to 100. The experimental running sum of the ( $p, t$ ) strengths in comparison to the QPM, SQPM and BCS calculations (*c*).

The strengths of the isoscalar and isovector quadrupole-quadrupole interactions in the SQPM,  $\kappa_{20}^{(0)}$  and  $\kappa_{20}^{(1)}$  respectively, were varied to fit the experimental energies and ( $p, t$ ) spectroscopic strengths of the lowest  $0^+$  states. It was found that an effect of

$\kappa_{20}^{(1)}$  on the ( $p, t$ ) spectroscopic strengths is negligible and that  $\kappa_{20}^{(0)}$  significantly influences the energy and spectroscopic strength of the first  $0^+$  excited state. It is known that in the even-even actinides the phonon coupling does not spoil the coherence of pairing correlations in the lowest  $0^+$  excited state [10]. As a consequence, the state has a pronounced pairing-vibrational character that manifests itself by large RPA backward  $\phi$  amplitudes. Fig. 5 shows that the contribution  $S_n^\phi(p, t)$  of the backward RPA amplitudes to the normalized relative transfer spectroscopic strength  $S_n(p, t)$  is important for the first excited  $0^+$  state, thus indicating its pairing vibrational character.

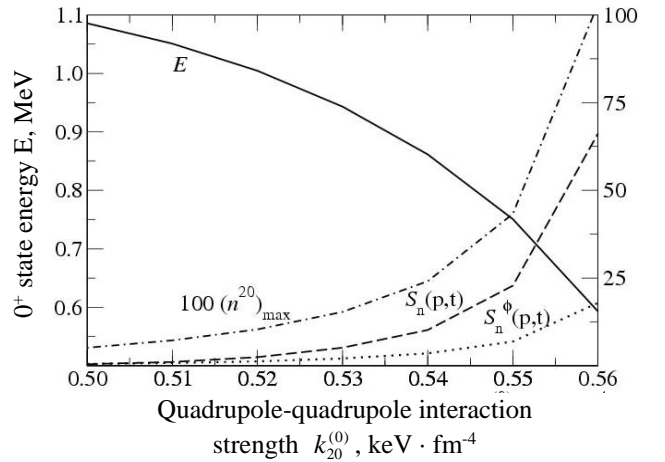


Fig. 5. The SQPM energy  $E$  (solid line), the normalized relative transfer strength  $S_n(p, t)$  (dashed line), the contribution  $S_n^\phi(p, t)$  of the backward RPA amplitude  $\phi$  to  $S_n(p, t)$  (dotted line) and the maximum number of quasiparticles with quantum number  $q$  in the ground state  $(n^{20})_{max}$  (dashed-dotted line) as functions of the isoscalar quadrupole-quadrupole interaction strength  $k_{20}^{(0)}$  for the first excited  $0^+$  state,  $k_{20}^{(1)} = 0$ .

The pairing interaction is essential for reproducing the experimental relative-transfer strength of the first excited  $0^+$  state. If we artificially lower the neutron and proton pairing interaction strengths, and simultaneously change the isoscalar quadrupole-quadrupole interaction to fit the experimental energy of the first excited  $0^+$  state, both  $S_n^\phi(p, t)$  and  $S_n(p, t)$  rapidly drop down. The SQPM predicts  $B(E2) = 4$  W.u. for the transition from the first excited  $0^+$  state to the  $2^+$  member of the g.s. band, the QPM gives a slightly low value of 2.3 W.u. Therefore, we can assume that the lowest  $0^+$  excited state ( $0^+_2$ ) has a mixed pairing-vibrational and  $\alpha$ -vibrational character. The contribution of  $S_n^\phi(p, t)$  for higher excited  $0^+$  states in the SQPM is significantly low and in most cases negligible, thus indi-



cating their weak phonon-vibrational or two-quasiparticle character. The maximum value of the number of quasiparticles with the quantum number  $q$  in the ground state,  $n_{max}^{20}$ , measures the ground-state correlations and can be calculated by using (see [34]):

$$n_{max}^{20} = \max \left[ \frac{1}{2} (\phi_{qq}^{20})^2 \right], \quad (10)$$

where  $\phi_{qq}^{20}$  are the backward RPA amplitudes of the first 0<sup>+</sup> excited state. For the isoscalar quadrupole-quadrupole interaction strength  $k_{20}^{(0)} = 0.554 \text{ keV} \cdot \text{fm}^{-4}$ , that reproduces the experimental energy of the first 0<sup>+</sup> excited state, the ground-state correlations estimated by  $n_{max}^{20}$  become large (see Fig. 5). As a consequence, the RPA approximation used in the SQPM is no more accurate and multi-phonon admixtures and interactions between phonons have to be taken into account.

In Fig. 4, *a* and *b* the experimental spectrum of the 0<sup>+</sup> (p, t) normalized relative transfer strengths is compared to the results of the SQPM and QPM calculations. The numerical results of the QPM calculations from [10] are provided to us by Sushkov [35]. Both SQPM and QPM calculations reproduce the

strong excitation of the first 0<sup>+</sup> excited state in accordance with the experiment. The SQPM generates 9 0<sup>+</sup> states below 2 MeV in fair agreement with the 10 firmly assigned states and 3 0<sup>+</sup> states in the region 2 - 3 MeV compared to 2 experimentally assigned states. The QPM fails to reproduce the experimental number of the 0<sup>+</sup> states. It predicts only 6 0<sup>+</sup> states below 2 MeV and 20 0<sup>+</sup> states in the region 2 - 3 MeV. The difference in the number of the 0<sup>+</sup> states between the SQPM and the QPM is caused mainly by the truncated SQPM model space (two-phonon states are not considered).

In Fig. 4, *c* we present also the increments of the experimental relative-transfer strength in comparison with those of the BCS, SQPM and QPM. Additional interactions in the QPM lead to level repulsion (excited 0<sup>+</sup> states spectrum broadening) and transfer strength fragmentation (lower relative transfer strength for the first excited 0<sup>+</sup> state in favor of higher excited states up to 2 MeV). In the region above 1.8 MeV, both SQPM and QPM fail to reproduce the sharp experimental increase of the (p, t) strength running sum.

**Table 3. Phonon structure of the QPM 0<sup>+</sup> states up to 2.6 MeV [35]. The weights of the one-phonon ( $\lambda\mu$ ) or the twophonon [ $(\lambda\mu)_i(\lambda\mu)_i$ ]-components are given in percent. Only main one-phonon and two-phonon components are shown. Transfer factors  $S(p, t)$  are normalized to 100 for the 0<sup>+</sup><sub>*g.s.*</sub>**

| $K_n^\pi$                    | $E_n(\text{calc}), \text{MeV}$ | $S(p, t)_{\text{calc}}$ | Structure  |
|------------------------------|--------------------------------|-------------------------|--|
| 0 <sup>+</sup> <sub>2</sub>  | 0.51                           | 25.81                   | (20) <sub>1</sub> 91   |
| 0 <sup>+</sup> <sub>3</sub>  | 1.33                           | 4.09                    | (20) <sub>2</sub> 90; [(22) <sub>1</sub> (22) <sub>1</sub> ] 4   |
| 0 <sup>+</sup> <sub>4</sub>  | 1.45                           | 4.01                    | (20) <sub>3</sub> 27; (20) <sub>5</sub> 27; [(22) <sub>1</sub> (22) <sub>1</sub> ]19; [(30) <sub>1</sub> (30) <sub>1</sub> ] 2                       |
| 0 <sup>+</sup> <sub>5</sub>  | 1.71                           | 0.03                    | (20) <sub>3</sub> 57; (20) <sub>5</sub> 23; (20) <sub>4</sub> 12   |
| 0 <sup>+</sup> <sub>6</sub>  | 1.79                           | 0.18                    | (20) <sub>4</sub> 79; [(22) <sub>1</sub> (22) <sub>1</sub> ] 3   |
| 0 <sup>+</sup> <sub>7</sub>  | 1.98                           | 4.64                    | (20) <sub>5</sub> 15; (20) <sub>7</sub> 15; (20) <sub>9</sub> 13; [(22) <sub>1</sub> (22) <sub>1</sub> ]16; [(30) <sub>1</sub> (30) <sub>1</sub> ] 4 |
| 0 <sup>+</sup> <sub>8</sub>  | 2.06                           | 1.59                    | (20) <sub>6</sub> 90   |
| 0 <sup>+</sup> <sub>9</sub>  | 2.14                           | 1.67                    | (20) <sub>7</sub> 55; (20) <sub>5</sub> 11; [(31) <sub>1</sub> (31) <sub>1</sub> ] 3; [(32) <sub>1</sub> (32) <sub>1</sub> ] 3                       |
| 0 <sup>+</sup> <sub>10</sub> | 2.29                           | 1.06                    | (20) <sub>9</sub> 49; (20) <sub>7</sub> 14; [(32) <sub>1</sub> (32) <sub>1</sub> ] 11  |
| 0 <sup>+</sup> <sub>11</sub> | 2.30                           | 0.06                    | (20) <sub>9</sub> 4; [(44) <sub>1</sub> (44) <sub>1</sub> ] 92   |
| 0 <sup>+</sup> <sub>12</sub> | 2.36                           | 0.11                    | (20) <sub>8</sub> 65; (20) <sub>12</sub> 16; [(30) <sub>1</sub> (30) <sub>1</sub> ] 2  |
| 0 <sup>+</sup> <sub>13</sub> | 2.43                           | 0.59                    | (20) <sub>10</sub> 7; [(32) <sub>1</sub> (32) <sub>1</sub> ] 65  |
| 0 <sup>+</sup> <sub>14</sub> | 2.48                           | 0.01                    | (20) <sub>10</sub> 63; (20) <sub>9</sub> 11; [(32) <sub>1</sub> (32) <sub>1</sub> ] 8  |
| 0 <sup>+</sup> <sub>15</sub> | 2.51                           | 1.73                    | (20) <sub>11</sub> 43; [(30) <sub>1</sub> (30) <sub>1</sub> ] 37   |
| 0 <sup>+</sup> <sub>16</sub> | 2.57                           | 3.55                    | (20) <sub>11</sub> 43; [(30) <sub>1</sub> (30) <sub>1</sub> ] 29   |

In Table 3 the structure and normalized relative-transfer strength of the QPM 0<sup>+</sup> excited states are presented. It is difficult to make an assignment to experimental levels above 1.5 MeV. The second two excited states, 0<sup>+</sup><sub>3</sub> and 0<sup>+</sup><sub>4</sub>, most probably correspond

to the experimental levels at 1.277 and 1.482 MeV, which is supported by the similar normalized relative transfer strengths. The experimental level at 0.927 MeV with the high  $B(E1)/B(E2)$  transition ratios and low normalized relative transfer strength is not re-

produced, neither in the SQPM (Table 4) nor in the QPM [10]. Contrary to the IBM, two-octupole phonon states are shifted to higher energies  $\sim 2.4 - 2.5$  MeV because to the Pauli exclusion principle. The lower-lying states (e.g.  $0_4^+$  at 1.45 MeV) possess only small two-octupole phonon admixtures. On the other hand, for the octupole-octupole isoscalar strength  $k_{30}^{(0)} = 7$  eV fm $^{-6}$ , that reproduces the experimental energy of the first  $1^-$  excited state, the SQPM predicts the enhanced  $E1$  transitions from the  $K = 0^-$  band to the g.s. band, e.g.  $B(E1; 1_1^- \rightarrow 0_1^+) = 0.2$  e $^2$ fm $^2 = 0.08$  W.u. As a consequence, even a small admixture of double octupole phonon configuration  $[(30)_1(30)_1]$  in  $0_3^+$  of about 0.3–0.6% can account for the experimentally observed  $B(E1)/B(E2)$  ratios (see Table 4).

**Table 4. Experimental and SQPM  $B(E1)/B(E2)$  transition ratios in  $^{232}\text{U}$  between the states of the  $0_3^+$  band and the  $0_1^-$  and  $0_1^+$  bands in units of  $10^{-4} \text{ b}^{-1}$**

| $K_i^\pi$ | $I_i$ | $I_{f1}$ | $I_{f2}$ | Exp.    | $B(E1)/B(E2)$ |
|-----------|-------|----------|----------|---------|---------------|
|           |       |          |          |         | SQPM          |
| $0_3^+$   | $0^+$ | $1_1^-$  | $2_1^+$  | 44(7)   | 7.5           |
|           | $2^+$ | $1_1^-$  | $0_1^+$  | 150(30) | 15            |
|           | $2^+$ | $1_1^-$  | $2_1^+$  | 45(1)   | 11            |
|           | $2^+$ | $1_1^-$  | $4_1^+$  | 24(1)   | 5.8           |
|           | $2^+$ | $3_1^-$  | $0_1^+$  | 337(68) | 23            |
|           | $2^+$ | $3_1^-$  | $2_1^+$  | 101(3)  | 16            |
|           | $2^+$ | $3_1^-$  | $4_1^+$  | 54(1)   | 8.8           |

The SQPM and the QPM are quite accurate in nuclei with small ground-state correlations. Since in  $^{232}\text{U}$  the ground-state correlations (as tested by the SQPM) become large, the effect of multi-phonon admixtures (three and more phonons) in the QPM that pushes two-phonon poles and consequently

two-phonon energies to lower values is then underestimated. In future QPM studies one also has to take into account the spin-quadrupole interaction, that is known to influence the density and structure of the low-lying  $0^+$  states [36].

## Conclusion

Firm assignments for the  $0^+$  state and most of the  $2^+$ ,  $4^+$  and for about half of the  $6^+$  states allowed to identify the sequences of states, which have the features of rotational bands with definite inertial parameters. Moments of inertia are derived from these sequences. Most of the values of the moments of inertia are not much higher than the value for the g.s. band. This indicates that they may correspond mainly to a quadrupolar one-phonon structure of  $0^+$  states.

The experimental data have been compared to the *spdf*-IBM and QPM calculations. The IBM reproduces the main characteristics of the experimental transfer distribution, namely the running sum of the (p, t) strengths and increased population of two groups of  $0^+$  excitations around 1 and 2 MeV, but the strength of the first excited  $0^+$  state is underestimated, and the strength of the second  $0^+$  state is overestimated. Most of the calculated excitations have two *pf* bosons in their structure, therefore being related to the presence of a double octupole structure. Good agreement with experiment for the  $B(E1)/B(E2)$  transition ratios indicates also the importance of the octupole degree of freedom. The QPM reproduces the strong (p, t) strength of the first excited  $0^+$  state due to its predicted pairing vibrational character and lower (p, t) strengths for higher-lying  $0^+$  states. It fails to account for a rapid increase of the running sum of the (p, t) strength above 1.8 MeV and predicts minor double-octupole phonon components in states below 2.4 MeV. Both models fail to give a detailed explanation of the individual states.

## REFERENCES

1. Leshner S. R., Aprahamian A., Trache L. et al. New  $0^+$  states in  $^{158}\text{Gd}$  // Phys. Rev. - 2002. - Vol. C 66. - P. 051305(R).
2. Meyer D.A., Wood V., Casten R.F. et al. Extensive investigation of  $0^+$  states in rare earth region nuclei // Phys. Rev. - 2006. - Vol. C 74. - P. 044309.
3. Bettermann L., Heinze S., Jolie J. et al. High-resolution study of  $0^+$  states in  $^{170}\text{Yb}$  // Phys. Rev. - 2009. - Vol. C 80. - P. 044333.
4. Ilie G., Casten R.F., von Brentano P. et al. Investigation of  $0^+$  states in  $^{192}\text{Pt}$  and  $^{194}\text{Pt}$  isotopes // Phys. Rev. - 2010. - Vol. C 82. - P. 024303.
5. Bernards C., Casten R.F., Werner V. et al. Investigation of  $0^+$  states in  $^{198}\text{Hg}$  after two-neutron pickup // Phys. Rev. - 2013. - Vol. C 87. - P. 024318.
6. Bucurescu D., Graw G., Hertenberger R. et al. High-resolution study of  $0^+$  and  $2^+$  excitations in  $^{168}\text{Er}$  with the (p, t) reaction // Phys. Rev. - 2006. - Vol. C 73. - P. 064309.
7. Levon A.I., Graw G., Eisermann Y. et al. Spectroscopy of  $^{230}\text{Th}$  in the (p, t) reaction // Phys. Rev. - 2009. - Vol. C 79. - P. 014318.
8. Levon A.I., Graw G., Hertenberger R. et al.  $0^+$  states and collective bands in  $^{228}\text{Th}$  studied by the (p, t) reaction // Phys. Rev. - 2013. - Vol. C 88. - P. 014310.
9. Lo Iudice N., Sushkov A.V., Shirikova N.Yu. et al. Microscopic structure of low-lying  $0^+$  states in the deformed  $^{158}\text{Gd}$  // Phys. Rev. - 2004. - Vol. C 70. - P. 064316.
10. Lo Iudice N., Sushkov A.V., Shirikova N.Yu. et al.

- Microscopic structure of low-lying  $0^+$  states in deformed nuclei // *Phys. Rev.* - 2005. - Vol. C 72. - P. 034303.
11. *Zamfir N.V., Jing-ye Zhang, Casten R.F. et al.* Interpreting recent measurements of  $0^+$  states in  $^{158}\text{Gd}$  // *Phys. Rev.* - 2002. - Vol. C 66. - P. 057303.
  12. *Sun Y., Aprahamian A., Jing-ye Zhang, Ching-Tsai Lee.* Nature of excited  $0^+$  states in  $^{158}\text{Gd}$  described by the projected shell model // *Phys. Rev.* - 2003. - Vol. C 68. - P. 061301(R).
  13. *Levon A.I., Graw G., Hertenberger R. et al.* Spectroscopy of  $^{232}\text{U}$  in the (p, t) reaction: Experimental data // *Yaderna fizyka ta energetyka (Nucl. Phys. At. Energy)*. - 2016. - Vol. 17, No. 3. - P. 215 - 226.
  14. *Browne E.* Nuclear Data Sheets for  $A = 232$  // *Nucl. Data Sheets*. - 2006. - Vol. 107. - P. 2579.
  15. *Weiss-Reuter R., Münzel H., Pfennig G.* Decay of  $^{232}\text{Np}$  // *Phys. Rev.* - 1972. - Vol. C6. - P. 1425.
  16. *Ardisson G., Hussonnois M., LeDu J.F. et al.* Levels of  $^{232}\text{U}$  Fed in  $^{236}\text{Pu}$   $\alpha$  Decay // *Phys. Rev.* - 1994. Vol. C 49. - P. 2963.
  17. *Spieker M., Bucurescu D., Endres J. et al.* Possible experimental signature of octupole correlations in the  $0^+_2$  states of the actinides // *Phys. Rev.* - 2013. - Vol. C 88. - P. 041303(R).
  18. *Iachello F., Arima A.* The Interacting Boson Model. - England, Cambridge: Cambridge University Press, 1987.
  19. *Engel J., Iachello F.* Interacting Boson Model of Collective Octupole States (I). The Rotational Limit // *Nucl. Phys.* - 1987. - Vol. A 472. - P. 61.
  20. *Zamfir N.V., Kusnezov D.* Octupole Correlations in the Transitional Actinides and the spdf Interacting Boson Model // *Phys. Rev.* - 2001. - Vol. C 63. - P. 054306.
  21. *Zamfir N.V., Kusnezov D.* Octupole correlations in U and Pu nuclei // *Phys. Rev.* - 2003. - Vol. C 67. - P. 014305.
  22. *Robledo L.M., Rodriguez-Guzman R.R.* Octupole deformation properties of actinide isotopes within a mean-field approach // *J. Phys. (London)* - 2012. - Vol. G 39. - P. 105013.
  23. *Robledo L.M., Butler P.A.* Quadrupole-octupole coupling in the light actinides // *Phys. Rev.* - 2013. - Vol. C 88. - P. 051302.
  24. *Nazarewicz W., Olanders P., Ragnarsson I. et al.* Analysis of Octupole Instability in Medium-Mass and Heavy Nuclei // *Nucl. Phys.* - 1984. - Vol. A 429. - P. 269.
  25. *Butler P.A., Nazarewicz W.* Intrinsic Reflection Asymmetry in Atomic Nuclei // *Rev. Mod. Phys.* - 1996. - Vol. 68. - P. 349.
  26. *Casten R.F., Warner D.D.* The interacting boson approximation // *Rev. Mod. Phys.* - 1988. - Vol. 60. - P. 389.
  27. *Kusnezov D.* The U(16) algebraic lattice. II. Analytic construction // *J. Phys.* - 1990. - Vol. A 23. - P. 5673.
  28. *Kusnezov D.* The U(16) algebraic lattice // *J. Phys.* - 1989. - Vol. A 22. - P. 4271.
  29. *Kusnezov D.* Computer code OCTUPOLE (unpublished).
  30. *Soloviev V.G.* Theory of Atomic Nuclei: Quasiparticles and Phonons. - Bristol: Institute of Physics, 1992.
  31. *Soloviev V.G.* Theory of Complex Nuclei. - Oxford: Pergamon Press, 1976.
  32. *Møller P., Nix J.R., Myers W.D., Swiatecki W.J.* Nuclear Ground-State Masses and Deformations // *Atomic Data Nucl. Data Tables*. - 1995. - Vol. 59. - P. 185.
  33. *Møller P., Nix J.R., Kratz K.-L.* Nuclear Properties for Astrophysical and Radioactive-Ion-Beam Applications // *Atomic Data Nucl. Data Tables*. - 1997. - Vol. 66. P. 131.
  34. *Weber T., de Boer J., Freitag K. et al.* Nuclear Levels in  $^{228}\text{Th}$  Populated in the Decay of  $^{228}\text{Pa}$  (II) // *Eur. Phys. J.* - 1998. - Vol. A3. - P. 25.
  35. *Sushkov A.V.* (Private communication).
  36. *Pyatov N.I.* Excitation of  $0^+$  states in two-particle transfer reactions // *Ark. Phys.* - 1967. - Vol. 36. - P. 667.

**О. І. Левон<sup>1</sup>, П. Алекса<sup>2</sup>, С. Паску<sup>3</sup>, П. Г. Тірольф<sup>4</sup>**

<sup>1</sup> Інститут ядерних досліджень, НАН України, Київ, Україна

<sup>2</sup> Інститут фізики та інститут чистих технологій,  
Технічний університет Острави, Чеська республіка

<sup>3</sup> Національний інститут фізики та ядерної інженерії ім. Г. Гулубея, Бухарест, Румунія

<sup>4</sup> Факультет фізики, Мюнхенський університет Людвіга-Максиміліана, Гархінг, Німеччина

### ДО ПРИРОДИ $0^+$ -ЗБУДЖЕННЯ В ДЕФОРМОВАНИХ ЯДРАХ АКТИНІДІВ

Спектри збудження в деформованому ядрі  $^{232}\text{U}$  досліджено в (p, t)-реакції. Тринадцять збуджених  $0^+$ -станів та інші стани зі спінами до  $6^+$  включно ідентифіковано при порівнянні експериментальних кутових розподілів тритонів і розрахунків у наближенні зв'язаних каналів. Побудовано послідовності збуджених станів, які можна трактувати як обертальні смуги. Моменти інерції визначено із цих послідовностей, що можуть розглядатись як свідчення дво- чи однофононої природи  $0^+$ -станів. Експериментальні дані порівнюються з розрахунками в рамках моделі взаємодіючих бозонів і квазічастинково-фононої моделі.

*Ключові слова:*  $0^+$ -стани, колективні смуги, моменти інерції, ядерні моделі.

**А. И. Левон<sup>1</sup>, П. Алекса<sup>2</sup>, С. Паску<sup>3</sup>, П. Г. Тирольф<sup>4</sup>**

<sup>1</sup> *Институт ядерных исследований, НАН Украины, Киев, Украина*

<sup>2</sup> *Институт физики и институт чистых технологий,  
Технический университет Остравы, Чешская республика*

<sup>3</sup> *Национальный институт физики и ядерной инженерии им. Г. Гулубея, Бухарест, Румыния*

<sup>4</sup> *Факультет физики, Мюнхенский университет Людвига-Максимилиана, Гархинг, Германия*

### **К ПРИРОДЕ $0^+$ -ВОЗБУЖДЕНИЙ В ДЕФОРМИРОВАННЫХ ЯДРАХ АКТИНИДОВ**

Спектры возбуждения в деформированном ядре  $^{232}\text{U}$  исследованы в (p, t)-реакции. Тринадцать возбужденных  $0^+$ -состояний и другие состояния со спинами вплоть до  $6^+$  идентифицированы из сравнения экспериментальных угловых распределений тритонов и вычислений в приближении связанных каналов. Построены последовательности возбужденных состояний, которые можно трактовать как вращательные полосы. Моменты инерции определены из этих последовательностей, которые могут рассматриваться как свидетельства двух- или одно-фононной природы  $0^+$ -состояний. Экспериментальные данные сравниваются с вычислениями в рамках модели взаимодействующих бозонов и квазичастично-фононной модели.

*Ключевые слова:*  $0^+$ -состояния, коллективные полосы, моменты инерции, ядерные модели.

Надійшла 03.08.2016

Received 03.08.2016